

**ELECTROCHEMICAL INVESTIGATION AND DIAGNOSIS
OF PERFORMANCE AND DURABILITY OF
PEM FUEL CELL CATHODE CATALYST LAYER**

SHANEETH M.



**DEPARTMENT OF CHEMICAL ENGINEERING
INDIAN INSTITUTE OF TECHNOLOGY DELHI**

OCTOBER 2018

© Indian Institute of Technology Delhi (IITD), New Delhi, 2018

**ELECTROCHEMICAL INVESTIGATION AND DIAGNOSIS
OF PERFORMANCE AND DURABILITY OF
PEM FUEL CELL CATHODE CATALYST LAYER**

by

SHANEETH M.

Department of Chemical Engineering

Submitted

in fulfilment of the requirements of the degree of Doctor of Philosophy
to the



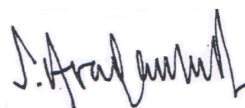
INDIAN INSTITUTE OF TECHNOLOGY DELHI

OCTOBER 2018

*Dedicated to my wife Bitha,
daughter Revathy
and our parents*

Certificate

This is to certify that the thesis entitled “**Electrochemical investigation and diagnosis of performance and durability of PEM fuel cell cathode catalyst layer**” submitted by **Mr. Shaneeth M.** to the Indian Institute of Technology Delhi, for the award of degree of doctor of philosophy, is a record of the original bonafide research work carried out by him. He has worked under our supervision and has fulfilled the requirements, which to our knowledge, has reached the requisite standard for the submission of this thesis. The results contained in this thesis have not been submitted in part or full to any University or Institute for the award of any degree or diploma.



(Dr. Suddhasatwa Basu)

Professor
Department of Chemical Engineering
Indian Institute of Technology Delhi
Hauz Khas, New Delhi 110 016

(Dr. Aravamuthan S.)

Outstanding Scientist & Deputy Director (Rtd.)
Vikram Sarabhai Space Centre
Indian Space Research Organisation
Thiruvananthapuram, Kerala 695 022

Acknowledgments

There is indeed a sense of joy and fulfilment while I write down this page! A work that engaged the mind for the last few years is now in black and white. Further, it gives immense pleasure to put on record the contributions from several people who guided, supported, encouraged, inspired and stood with me.

First and foremost, I express my sincere gratitude to my supervisors, **Dr. Suddhasatwa Basu** and **Dr. S. Aravamuthan** who guided and supervised me throughout the duration of this work. Their comments and guidance improved the work a lot and they provided the freedom, advices, support and motivation in abundance; and most importantly, when and where those were needed. Thanks are to both of them and for their patience and trust.

I am grateful to VSSC management for providing necessary permission for doing this work.

I am thankful to all the Professors who were in the chair of Head of the Department, Dept. of Chemical Engineering, IIT Delhi during the period of my work at IIT, Delhi. They were always there to provide required help. I am grateful to my Deputy Director at VSSC, Dr. S. C. Sharma for the freedom he has given me to fix priorities, while there were several other pressing tasks.

Similarly my seniors at VSSC, Thiruvananthapuram who headed my division or entity from time to time, played a very important role in enabling me to carry on with my research work and they continue to motivate. Ms. Mercy T. D., present Head of Energy System Division, Shri. Kamalakaran K. P., former Head of Lithium-ion and Fuel Cell Division and Shri. Raveendran Pillai former Head of Battery Development Division, keep prompting and encouraging me with sisterly/brotherly affection. Also are other former seniors, Shri. M. J. Nair, Ms. M. N. Radhakumari, Shri. P. R. Nair and Shri. B. Velayudham who

understood my passion for Fuel Cells and readily extended the needed support; without their help, I wouldn't have got the opportunity to think about pursuing this work in this form.

Hearty thanks to my thesis committee members at IIT Delhi and the academic committee members at VSSC for the valuable suggestions and criticisms; they enriched my thesis greatly.

A work of this kind is impossible without the support of my dearest colleagues who literally created the required environment for this work in Fuel cell lab at VSSC that normally works for products. I am indebted to Ms. Remya K.P, Shri. Vipin V. and Shri. Remesh S. for the meticulous manner in which they ensured the work related to the long and numerous processing and testing activities were completed, in accordance with my plans. I also owe Shri. Rajeshkumar K, Shri. Rajeshkumar R. and Shri. Manu for their company during holidays and Ms. Jeena and Dr. Desikan for all the help towards facilitating review of thesis manuscripts by my supervisor!

Special thanks are to the rest my colleagues in Fuel Cell lab at VSSC, Shri. Surajeet Mohanty, Shri. Vinay Mohan Bhardwaj, Shri. Samrat Deb Choudhury, Shri. Nandikesan P. and Shri. Vishnugopal who too helped me to create and sustain the environment for this work amidst several priorities; it was indeed interesting to discuss the research outcome, from time to time. Thanks are also to Shri. Harikumar and Shri. Thomas. Special thanks are to Ms. Abha Bharti who provided Pt-TiO₂ material for my study. Thanks are due to Shri. Manojkumar C. K., who was part of the fuel cell lab in the initial period and who helped in conducting the experiment.

Thanks are to Ms. Bhuvaneshwari and Ms. Jayalatha of ASD/VSSC and Shri. Sushant of MCD/VSSC for their support for physical characterisation of materials. Thanks are also to

Dr. Rajeev R., Head, ASD, Dr. Benny George, GD, ASCG and Dr Ramesh Narayan, Head, MCD.

Dr. Varagunapandiyan and Shri. Harikrishnan N. of Fuel Cell lab, IIT Delhi took care of my needs at IIT Delhi while I was working at VSSC; also, I received ample support at different points of time from Dr. Rajalakshmi,, Dr. Pankaj, Dr. Gurpreet, Ms. Jyotsna Annepu, Dr. Amandeep, Shri. Anuj and Shri. Sundar during my stay at IIT Delhi and enjoyed their company. Thanks are to all of them.

Fondly remember with thanks our Devu valyamma, who is not there with us today; she was the first to offer help and the one who readily came forward to support my family during my absence from home for studies at IIT and my in-laws for their constant encouragement and care. Thanks are also to my sister, Nisheetha, my best ever academic buddy, and her family for their motivation.

A big salute to my parents, Shri. Sreedharan and Smt. Sobhana, because of whom what I am today, and to all my teachers, mentors, friends and well-wishers since childhood, whose advices and wisdom keep on moulding me.

To my wife Bitha and my daughter Revathy, it's their work as well since this thesis was 'the priority' to all of us; hence, our life was certainly different in the last few years. We note it and hope our priorities continue to provide us satisfaction.

Finally, thanks are to all who have directly and indirectly helped me during various stages of this work, whom I might have missed to mention here.

Shaneeth M.

Abstract

PEM fuel cell has emerged as a key solution in the emerging renewable energy scenario. It offers zero-emission-fuel driving capability with highest energy conversion efficiency along with a host of other benefits in diverse applications. However, cathode catalyst durability of PEM Fuel Cell is a major concern today. In this work, an in-situ Accelerated Durability Test cum Diagnostic Analysis Protocol (ADT-DAP) based on electrochemical techniques is developed towards studying performance and durability of cathode catalyst. The protocol so developed is applied to various cases of relevance to PEM Fuel Cell and its capability to derive significant inferences is demonstrated for 10,000 cycles long potential cycling tests.

The protocol developed is designed to de-convolute various types and classes of losses pertaining to different electrode elements. With this, the changes in the catalytic activity under true in-situ conditions are assessed. The changes in the cathode catalyst layer (CCL) with regard to electrochemical surface area (ECSA), support surface area characteristics, catalyst layer resistance, transport resistance and kinetic parameters are computed and compared for various cases. A salient feature of the work is that EIS carried out under non-charge transfer conditions is used for the purpose. The protocol is demonstrated to be a more deterministic and powerful and more reliable tool than conventional cyclic voltammetry based durability diagnostics. The results thus obtained are interpreted further along with the post-test physical characterisation of the catalyst material involving XRD, Raman spectroscopy and SEM techniques. which involves an element of subjectivity.

Specific cases studies selected include design and process changes in electrodes, Pt catalysts with different supports and CCLs under varying test conditions. Pt loading in the range of 0.07 to 0.37 mg/cm² indicated variations in utilisation of Pt, catalyst layer resistance and the extent of reduction of ECSA. Similarly, the electrode process changes in terms electrode pressing

temperature and varying catalyst coating processes have brought out the differences in the catalyst layer ohmic resistance as well as ECSA reduction characteristics. Study involving carbon and TiO₂ supports has revealed the contrast in stability of the Pt particles over the respective supports. Support by itself was found to have similar degradation characteristics, however, stability of Pt on respective supports were found to be significantly different. Different test conditions involving upper limit of potential in the range of 1.0 V to 1.4 V formed another case study. Increase in ECSA reduction along with increase in upper potential limit is noted. Carbon support is found to undergo graphitisation due to cycling and, possibly as a result of it, Pt is found to be getting unstable on the support. In the cases studied, exchange current density values computed from the results indicated increasing trend with cycling. Also, with cycling, Pt crystallite size is found to be growing in size and, it is inferred that, this is due to dissolution-recrystallization.

The in-situ Accelerated Durability Test cum Diagnostic Analysis Protocol (ADT-DAP) developed is found to provide quite comprehensive in-sights into degradation characteristics of cathode catalyst layer under varying conditions.

Key words: PEM, Fuel Cell, durability, polarisation, limiting current, EIS, XRD, degradation, catalyst layer, recrystallization, crystallites, lattice, ECSA, Pt, SEM, FESEM, Raman spectroscopy

सार

पीईएम ईंधन सेल उभरते अक्षय ऊर्जा परिदृश्य में एक महत्वपूर्ण समाधान के रूप में उभरा है। यह विविध अनुप्रयोगों में अन्य लाभ के एक मेजबान के साथ उच्चतम ऊर्जा रूपांतरण दक्षता के साथ शून्य उत्सर्जन ईंधन ड्राइविंग क्षमता प्रदान करता है। हालांकि, पीईएम ईंधन सेल के कैथोड उत्प्रेरक स्थायित्व एक प्रमुख चिंता का विषय आज कर रहा है। इस काम में, एक इन-सीटू त्वरित टिकाऊपन टेस्ट सह नैदानिक विश्लेषण प्रोटोकॉल (ADT-डीएपी) विद्युत तकनीक पर आधारित कैथोड उत्प्रेरक के प्रदर्शन और स्थायित्व का अध्ययन की दिशा में विकसित की है। प्रोटोकॉल इतना विकसित विभिन्न मामलों पर लागू होता है पीईएम ईंधन सेल की प्रासंगिकता और महत्वपूर्ण संदर्भ प्राप्त करने की इसकी क्षमता 10,000 चक्र लंबे संभावित साइकिल चलाना परीक्षणों के लिए प्रदर्शित की जाती है।

प्रोटोकॉल विकसित विभिन्न प्रकार और विभिन्न इलेक्ट्रोड तत्वों से संबंधित नुकसान की कक्षाओं को डी-कुंडलित बनाया गया है। इसके साथ ही सही इन-सीटू की शर्तों के तहत उत्प्रेरक गतिविधि में परिवर्तन का आकलन किया जाता है। कैथोड उत्प्रेरक परत (सीसीएल) के साथ में परिवर्तन काम की मोक्ष की विशेषता यह है कि गैर-चार्ज स्थानांतरण स्थितियों के तहत किए गए ईआईएस का उपयोग किया जाता है इस प्रयोजन के लिए। प्रोटोकॉल पारंपरिक चक्रीय voltammetry आधारित स्थायित्व निदान की तुलना में अधिक नियतात्मक और शक्तिशाली और अधिक विश्वसनीय उपकरण का प्रदर्शन किया है। इस प्रकार प्राप्त परिणामों XRD, रमन को शामिल उत्प्रेरक सामग्री के बाद परीक्षण शारीरिक लक्षण वर्णन के साथ साथ आगे व्याख्या कर रहे हैं स्पेक्ट्रोस्कोपी और एसईएम तकनीकें जिनमें विषयपरकता का एक तत्व शामिल है।

/ सेमी 2 पं का उपयोग, उत्प्रेरक परत प्रतिरोध और की हद में बदलाव का संकेत दिया विशिष्ट मामलों चयनित पढ़ाई परीक्षण की स्थिति। 0.07 0.37 मिलीग्राम की सीमा में पं लोड हो रहा है बदलती के तहत इलेक्ट्रोड में डिजाइन और प्रक्रिया में बदलाव, विभिन्न समर्थन करता है के साथ पं उत्प्रेरक और CCLs शामिल ECSA की कमी। इसी तरह, संदर्भ इलेक्ट्रोड में इलेक्ट्रोड प्रक्रिया परिवर्तन तापमान दबाकर और उत्प्रेरक कोटिंग प्रक्रियाओं बदलती बाहर ओमिक प्रतिरोध उत्प्रेरक परत में अंतर के साथ-साथ ECSA कमी विशेषताओं लाया है। अध्ययन से जुड़े कार्बन और TiO₂ स्थिरता में विपरीत पता चला है का समर्थन करता है संबंधित समर्थन करता है से अधिक पं कणों की। अपने आप में समर्थन समान गिरावट विशेषताओं पाया गया है, तथापि, पं संबंधित समर्थन करता है पर की स्थिरता काफी अलग पाए गए। 1.0 वी की रेंज में संभावित की ऊपरी सीमा से जुड़े विभिन्न परीक्षण की स्थिति 1.4 वी ने एक अन्य केस स्टडी का गठन किया। के साथ ईसीएसए में कमी में वृद्धि ऊपरी संभावित सीमा में ncrease विख्यात है। कार्बन समर्थन संभवतः इसके बारे में एक परिणाम के रूप में साइकिल चलान के कारण graphitisation गुजरना करने के लिए और, पाया जाता

है, पंडित, समर्थन पर अस्थिर हो रही पाया जाता है। मामलों का अध्ययन किया विनिमय वर्तमान घनत्व की गणना मूल्यों परिणाम साइकिल चालन के साथ प्रवृत्ति में वृद्धि का संकेत दिया। इसके अलावा, साइकिल चलाना साथ, पंडित स्फटिक आकार पाया जाता है आकार में बढ़ती जा करने के लिए और, यह पता चलता है कि, इस विघटन-recrystallization के कारण है।

इन-सीटू त्वरित टिकाऊपन टेस्ट सह नैदानिक विश्लेषण प्रोटोकॉल (ADT-डीएपी) विकसित की बदलती परिस्थितियों में कैथोड उत्प्रेरक परत का क्षरण विशेषताओं में इन-स्थलों काफी व्यापक प्रदान करने के लिए पाया जाता है।

कुंजी शब्द: पीईएम, ईंधन सेल, स्थायित्व, ध्रुवीकरण, वर्तमान सीमित, EIS, XRD, गिरावट, उत्प्रेरक परत, recrystallization, crystallites, जाली, ECSA, पंडित, SEM, FESEM, रमन स्पेक्ट्रोस्कोपी

Table of Contents

	Page No.
<i>Certificate</i>	i
<i>Acknowledgement</i>	iii
<i>Abstract</i>	vii
<i>Table of contents</i>	ix
<i>List of figures</i>	xv
<i>List of tables</i>	xxi
<i>List of symbols</i>	xxiii
Chapter 1: Introduction and literature review	1
1.1 Background	1
1.1.1 Emerging energy scenario and Proton Exchange Membrane (PEM) fuel cells	1
1.1.2 PEM fuel cell technology targets and durability	2
1.2 Literature review	5
1.2.1 The Cathode Catalyst Layer (CCL) and its durability	5
1.2.2 CCL durability mitigation	10
1.2.3 Accelerated Durability Test (ADT) protocols	13
1.2.4 Cathode catalyst layer diagnostics	14
1.2.5 EIS based CCL degradation studies	18
1.2.6 Diagnosing gas transport resistance	19

1.3	Motivation and gap analysis	20
1.4	Objectives of the thesis	23
1.5	Thesis organisation	24
Chapter 2: The methodology for electrochemical investigation of performance and durability of PEM fuel cell cathode catalyst layer		27
2.1	Introduction	27
2.2	Electrochemical diagnostic analysis of cathode catalyst layer	29
2.2.1	EIS based ECSA estimation	29
2.2.2	Catalyst layer resistance from impedance plots	34
2.2.3	Gas transport resistance	37
2.2.4	Tafel Analysis	38
2.3	The Accelerated Durability Test cum Diagnostic Analysis protocol (ADT-DAP)	41
2.3.1	The experimental setup for electrochemical accelerated durability test cum diagnostics	41
2.3.2	The experimentation scheme for electrochemical durability test and diagnostics	43
2.4	Uncertainty analysis	46
2.5	Summary of the work methodology for electrochemical investigation of CCL	47
Chapter 3: Investigation of cathode catalyst layer Pt loading level and processes with respect to performance & durability		49
3.1	Introduction	49
3.2	Investigation of cathode catalyst layer Pt loading levels	53

3.2.1	Experimental details of the studies on Pt loading level in CCL	53
3.2.2	Results and discussions of the studies on Pt loading levels in CCL	54
3.2.2.1	Electrochemical test results and discussion on CCL Pt loading	54
3.2.2.2	Physical characterisation results and discussions on CCL Pt loading	69
3.2.3	Summary of the studies on CCL Pt loading level	71
3.3	Investigation of Membrane Electrode Assembly hot pressing (MEA) temperature	71
3.3.1	Experimental details of the study on MEA hot pressing temperature	71
3.3.2	Results and discussion on the study of MEA hot pressing temperature	72
3.3.3	Summary of the studies on MEA hot pressing temperature	74
3.4	Investigation of different catalyst coating processes for CCL	75
3.4.1	Experimental details of the study on coating processes for CCL	75
3.4.2	Results and discussion of the study on coating processes for CCL	76
3.5	Summary of the investigation on cathode catalyst layer Pt loading levels and processes	80

Chapter 4: Investigation of performance and durability of Carbon and TiO₂ supported Pt based cathode catalyst layers	83
4.1 Introduction	83
4.2 Experimental details of the studies on Carbon and TiO ₂ supported Pt based CCLs	87
4.3 Results and discussions on the study of Carbon and TiO ₂ support based CCLs	89
4.3.1 Electrochemical diagnostic results & discussions on C and TiO ₂ support based CCLs	89
4.3.2 Physical characterisation results and discussions on C & TiO ₂ support based CCLs	107
4.4 Summary of the investigations on Carbon and TiO ₂ supported Pt based cathode catalyst layers	111
Chapter 5: Investigation of carbon supported Pt based cathode catalyst layer durability under potential cycling test with different voltage limits	113
5.1 Introduction	113
5.2 Experimental details of the study on potential cycling tests with different voltage limits	115
5.3 Results and discussions of the study on potential cycling tests with different voltage limits	117
5.3.1 Electrochemical diagnostics results and discussions on Pt-C based CCLs under potential cycling test	117
5.3.2 Physical characterisation results and discussion on Pt-C based CCLs under potential cycling test	134
5.4 Summary of the investigation of CCLs under potential cycling test	139

Chapter 6: Summary and Conclusions and Future Directions	140
6.1 Summary	140
6.2 Conclusions	144
6.3 Future directions	146
References	147
Curriculum Vitae	169

List of Figures

Figure No.	Title	Page No.
Fig. 1.1	Schematic of a typical PEM Fuel Cell	4
Fig. 1.2	Representation of different types of losses in a PEM Fuel cell	6
Fig. 1.3	Schematic of Cathode catalyst layer: (a) overall CCL structure with various	8
Fig. 1.4	Electrical circuit model of a catalyst layer	9
Fig. 2.1	Typical CV obtained with a cell having 20%Pt-C cathode/pure Pt anode under hydrogen on anode and argon gas on cathode	30
Fig. 2.2	Typical CV with the potential window for EIS marked	31
Fig. 2.3	Nyquist plots (A) and the capacitance plots (B) typically obtained at potentials corresponding to HAD and DL regions of 20%Pt-C cathode/pure Pt anode with Hydrogen on anode and Argon gas on cathode	32
Fig. 2.4	Schematic of the finite transmission line equivalent circuit considered	35
Fig. 2.5	Typical Nyquist plot at double layer region with graphical representation of resistance measurement	36
Fig. 2.6	The i-V curve obtained during a typical limiting measurement test	37
Fig. 2.7	The experimental set-up fabricated and used for conducting the electrode performance and durability test of PEM Fuel Cells	42
Fig. 2.8	Typical potentiostatic characteristics during a “purge PST” cycle	44
Fig. 2.9	The schematic of the accelerated durability test cum diagnostic analysis protocol: (a) Overall test flow and (b) specific tests and the linkages	45

Fig. 3.1	Nyquist plots obtained at 100 th cycle (BOL) for 20% Pt-C based cathodes of different Pt loading at HAD regime	55
Fig. 3.2	Nyquist plots obtained at 100 th cycle (BOL) for 20% Pt-C based cathodes of different Pt loading at HAD regime	55
Fig. 3.3	Capacitance plots obtained from EIS data at 100 th cycle (BOL) for 20% Pt-C based cathodes with different Pt loading at HAD regime	56
Fig. 3.4	Capacitance plots obtained from EIS data at 100 th cycle (BOL) for 20% Pt-C based cathodes with different Pt loading at DL regime	56
Fig. 3.5	Effect of cathode Pt loading level on limiting capacitance at HAD for different potential cycles.	57
Fig. 3.6	Effect of Pt loading level of 20% Pt-C based cathodes on limiting capacitance at DL for different potential cycles	58
Fig. 3.7	Effect of Pt loading of 20% Pt-C based cathodes on limiting capacitance due to active Pt for varying potential cycles.	59
Fig. 3.8	Effect of Pt loading of 20% Pt-C cathodes on ECSA for different potential cycles	60
Fig. 3.9	Effect of Pt loading on % ECSA for varying potential cycles for 20% Pt-C based cathodes	61
Fig. 3.10	Effect of potential cycling on ECSA at varying Pt loading for 20% Pt-C cathodes	62
Fig. 3.11	Effect of cycling on limiting capacitance due to active Pt for varying loading level 20% Pt-C based cathode	63
Fig. 3.12	Effect of cycling on limiting capacitance at double layer regime for varying Pt loading on 20% Pt-C based cathode.	63
Fig. 3.13	Effect of cycling on % ECSA for varying Pt-loading on 20% Pt-C based cathode	64
Fig. 3.14	Effect of cycling on % surface area with regard to varying Pt-loading level of 20% Pt-C based cathodes	65
Fig. 3.15	Effect of potential cycling on catalyst layer resistance for different Pt loading in 20% Pt-C based cathodes	66

Fig. 3.16	Effect of Pt loading on catalyst layer resistance in 20% Pt-C based cathodes for different potential cycles	67
Fig. 3.17	HFR values at different stages of potential cycling for electrodes with different Pt loading in 20% Pt-C based cathodes	68
Fig. 3.18	HFR values of electrodes with different Pt loading in 20% Pt-C based cathodes at different stages of potential cycling	68
Fig. 3.19	SEM images of 20% Pt-C based cathodes with different catalyst loading (as coated)	70
Fig. 3.20	Comparison of effect of cycling on ECSA of 20% Pt-C based cathodes processed through different hot pressing temperature levels.	72
Fig. 3.21	Effect of cycling on catalyst layer resistance of 20% Pt-C based cathodes processed through different hot pressing temperature levels.	73
Fig. 3.22	Effect potential cycling on normalised catalyst layer resistance of 20% Pt-C based cathode of electrodes processed at different hot pressing temperature levels.	72
Fig. 3.23	Effect of potential cycling on ECSA for 20% Pt-C based cathodes processed using screen printing and spray coating methods.	76
Fig. 3.24	Effect of potential cycling on catalyst layer resistance of 20% Pt-C based cathodes processed using two methods, viz., screen printing and spray coating.	77
Fig. 3.25	Effect of coating process and cycling on overall transport resistance values of cathodes based on 20% Pt-C	78
Fig. 3.26	SEM images of the two types of cathodes based on 20% Pt-C, coated via Screen printing and spray coating (as coated)	79
Fig. 4.1	Polarisation characteristics of (a) Pt-C and (b) Pt-TiO ₂ based PEM fuel cells, obtained periodically during cycling test	90
Fig. 4.2	EIS spectra obtained at Hydrogen adsorption/desorption (HAD) region with anode under hydrogen and cathode under argon in the frequency range of 0.1 to 100 kHz for PEM fuel cells with (a) 20% Pt-C and (b) 20% Pt-TiO ₂ based CCLs, obtained periodically during cycling test.	91

Fig. 4.3	EIS spectra obtained at double layer (DL) region with anode under hydrogen and cathode under argon in the frequency range 0.1 to 100 kHz for PEM fuel cells with (a) 20% Pt-C and (b) 20% Pt-TiO ₂ based CCLs, obtained periodically during cycling test.	92
Fig. 4.4	Capacitance plots derived from the electrochemical impedance spectra from the hydrogen adsorption/desorption region with anode under hydrogen and cathode under argon in the frequency range 0.1 to 100 kHz for PEM fuel cells with (a) 20% Pt-C and (b) 20% Pt-TiO ₂ based CCLs, obtained periodically during cycling test.	93
Fig. 4.5	Capacitance plots derived from the electrochemical impedance spectra obtained at the double layer region with anode under hydrogen and cathode under argon in the frequency range 0.1 to 100 kHz for PEM fuel cells with (a) 20% Pt-C and (b) 20% Pt-TiO ₂ based CCLs, obtained periodically during cycling test.	94
Fig. 4.6	Electrochemical surface area (ECSA) variations on the cathode side of the PEM fuel cells with (a) 20% Pt-C and (b) 20% Pt-TiO ₂ based CCLs, obtained periodically during cycling test.	95
Fig. 4.7	Effect of cycling on normalised area of Pt support on the cathode side of PEM fuel cells with (a) 20% Pt-C and (b) 20% Pt-TiO ₂ based CCLs, obtained periodically during cycling test.	96
Fig. 4.8	Resistance of the cathode catalyst layer of PEM fuel cells with (a) 20% Pt-C and (b) 20% Pt-TiO ₂ based CCLs, obtained periodically during cycling test.	98
Fig. 4.9	Over potentials due to catalyst layer resistance at the cathode of PEM fuel cells with (a) 20% Pt-C and (b) 20% Pt-TiO ₂ based CCLs, obtained periodically during cycling test.	99
Fig. 4.10	High Frequency Resistance (HFR) as computed from EIS spectra of cells with (a) 20% Pt-C and (b) 20% Pt-TiO ₂ based CCLs, obtained periodically during cycling test.	100
Fig. 4.11	Over potentials due to Internal Resistance / High Frequency Resistance (HFR) for the cells with (a) 20% Pt-C and (b) 20% Pt-TiO ₂ based CCLs, obtained periodically during cycling test.	101
Fig. 4.12	Total mass transport resistance of the cathode of the cells with (a) 20% Pt-C and (b) 20% Pt-TiO ₂ based CCLs, obtained periodically during cycling test.	102

Fig. 4.13	Mass transport over potentials at the cathode of the cells with (a) 20% Pt-C and (b) 20% Pt-TiO ₂ based CCLs, obtained periodically during cycling test.	103
Fig. 4.14	Corrected cell potentials of the cells with (a) 20% Pt-C and (b) 20% Pt-TiO ₂ based CCLs with current density scaled to net available Pt area.	104
Fig. 4.15	Effect of cycling on (a) Tafel slope and (b) exchange current density of the cathode side of cells with (a) 20% Pt-C and (b) 20% Pt-TiO ₂ based CCLs, obtained periodically during cycling test.	106
Fig. 4.16	XRD pattern of the catalyst materials of (a) 20% Pt-C and (b) 20% Pt-TiO ₂ based cathodes, before and after cycling	108
Fig. 4.17	Difference between (a) 2 Θ and (b) d-space values corresponding to the XRD peaks of various Pt crystal systems of cycled and uncycled Pt-C and Pt-TiO ₂ based cathode catalyst material.	110
Fig. 5.1	Effect of potential cycling with different upper voltage limit on polarisation characteristics of cells with 20% Pt-C based CCLs: (a) 1.0 V, (b) 1.2 V and (c) 1.4 V	118
Fig. 5.2	Effect of potential cycling with different upper voltage limit on cyclic voltammogram of the three cells with 20% Pt-C based CCL, after 100th cycle and 10, 000th cycle: (A) 1.0 V, (B) 1.2 V and (C) 1.4 V	119
Fig. 5.3	Nyquist plots of the three cells obtained at HAD region for the three cells with 20% Pt-C based CCL at varying stages of cycling: (a) 1.0 V, (b) 1.2 V and (c) 1.4 V	121
Fig. 5.4	Nyquist plots of the three cells obtained at DL region for the three cells with 20% Pt-C based CCL at varying stages of cycling: (a) 1.0 V, (b) 1.2 V and (c) 1.4 V	122
Fig. 5.5	Capacitance plots of the three cells obtained at HAD region for the three cells with 20% Pt-C based CCL at varying stages of cycling: (a) 1.0 V, (b) 1.2 V and (c) 1.4 V	124
Fig. 5.6	Capacitance plots of the three cells obtained at DL region for the three cells with 20% Pt-C based CCL at varying stages of cycling: (a) 1.0 V, (b) 1.2 V and (C) 1.4 V	125

Fig. 5.7	Effect of potential cycling on ECSA of the three cells for the three cells with 20% Pt-C based CCL	126
Fig. 5.8	Normalised ECSA values of the three cells for the three cells with 20% Pt-C based CCL at varying stages of cycling	127
Fig. 5.9	Effect of potential cycling on catalyst layer resistance of the three cells with 20% Pt-C based CCL	127
Fig. 5.10	Effect of cycling at different upper voltage limits on HFR for the three cells with 20% Pt-C based CCL.	129
Fig. 5.11	Effect of potential cycling on total surface area of the catalyst layer for the three cells with 20% Pt-C based CCL with different voltage limits	130
Fig. 5.12	Effect of potential cycling on transport resistance in the catalyst layer for the three cells with 20% Pt-C based CCL	131
Fig. 5.13	Normalised transport resistance of the cathode catalyst layer for the three cells with 20% Pt-C based CCL at varying stages of cycling	132
Fig. 5.14	Effect of cycling on exchange current density (a) and Tafel slopes (b) of Pt in cathodes of the three cells with 20% Pt-C based CCL at different voltage limits.	133
Fig. 5.15	Raman spectra of the catalyst materials of CCL of the three cells with 20% Pt-C based CCL, cycled to different voltage limits.	134
Fig. 5.16	XRD pattern of the catalyst materials of CLL of the three cells with 20% Pt-C based CCL, cycled to different voltage limits.	135
Fig. 5.17	FESEM images of cathode catalyst layer morphology at different stages of cycling	138

List of Tables

Table No.	Title	Page No.
Table 5.1	Pt crystallite parameters of Pt[111] as obtained from XRD characterization	136

List of symbols

Latin symbols

Symbol	Parameter	Value	Unit
C_{FHAD}	Faradaic capacitance at the hydrogen adsorption and desorption region		mF.cm^{-2}
C_{TDL}	Total capacitance at the double layer region		mF.cm^{-2}
C_{THAD}	Total capacitance at the hydrogen adsorption and desorption region		mF.cm^{-2}
C_{O_2}	Concentration of O_2		mol.m^{-3}
E_{cell}	Cell potential (measured)		V
E_{corr}	Cell potential corrected for resistive and transport losses		V
E_{rev}	Reversible potential	1.228	V
F	Faraday's constant	96485	C.mol^{-1}
I	Current		A
i	Current density		$\text{A.cm}^{-2}_{\text{geo}}$
i_0	Exchange current density		$\text{A.cm}^{-2}_{\text{Pt}}$
i_{lim}	Limiting current density		$\text{A.cm}^{-2}_{\text{geo}}$
k_{DL}	Specific capacitance at the double layer region		F.m^{-2}
k_{HAD}	Specific capacitance at the Hydrogen adsorption/desorption region	12.95	F.m^{-2}
L_{CS}	Catalyst support loading		$\text{mg}_{\text{CS}}.\text{cm}^{-2}_{\text{geo}}$
L_{Pt}	Platinum loading		$\text{mg}_{\text{Pt}}.\text{cm}^{-2}_{\text{geo}}$
$P_{\text{O}_2, \text{channel}}$	O_2 partial pressure in the flow field channel		Pa

Q_{HAD}	Total charge due to hydrogen adsorption and desorption phenomena		C.cm^{-2}
R	Universal gas constant	8.314	$\text{J.mol}^{-1}.\text{K}^{-1}$
R_{ACLR}	Cathode catalyst layer resistance		$\Omega.\text{cm}^2$
R_{CCLR}	Cathode catalyst layer resistance		$\Omega.\text{cm}^2$
R_{HFR}	High frequency resistance		Ω
$R_{\text{O}_2 \text{ trans total}}$	Total Oxygen gas transport resistance		s.cm^{-1}
T	Temperature		K
S_{CS}	Surface area of catalyst support		$\text{m}^2.\text{g}^{-1}\text{CS}$
S_{Pt}	Surface area of active Pt (Electrochemical surface areas)		$\text{m}^2.\text{g}^{-1}\text{Pt}$

Greek symbols

Symbol	Parameter	Value	Unit
α	Transfer coefficient	1	
γ	ORR reaction order with respect to p_{O_2}	0.548	
η_{ACLR}	Over potential due to anode catalyst layer resistance		V
η_{CCLR}	Over potential due to cathode catalyst layer resistance		V
η_{HFR}	Over potential due to anode high frequency resistance		V

η_{HOR}	Over potential due to HOR	V
η_{ORR}	Over potential due to OOR	V
$\eta_{\text{H2 transport}}$	Over potential due to resistance to Hydrogen gas transport	V
$\eta_{\text{O2 transport}}$	Over potential due to resistance to Oxygen gas transport	V
Σ	Three times the difference between real axis intercepts at high frequency and the tangent to the low frequency capacitive line in Nyquist plot (Catalyst layer resistance)	$\Omega.\text{cm}^2$